British Journal of Nutrition (2010), **104**, 291–297
doi:10.1017/S0007114510000450

Mechanism of impaired baroreflex sensitivity in Wistar rats fed a high-fat and -carbohydrate diet

Jing Ai, Feng Liang, Hongyu Zhou, Jing Zhao, Ning Wang, Songling Zhu and Baofeng Yang*

Department of Pharmacology, and the State-Province Key Laboratory of Biomedicine and Pharmaceutics, Harbin Medical University, Harbin 150081, China

(Received 19 June 2009 – Revised 14 January 2010 – Accepted 18 January 2010 – First published online 1 March 2010)

Both high-fat and high-carbohydrate diets have been considered in association with the impairment of baroreflex sensitivity. However, the mechanisms are unclear. In the present study, the effects of a complex high-fat and high-carbohydrate diet (HFCD) on baroreflex circuitry were investigated. A HFCD emulsion was formulated and orally administered to rats for 30 d. Rats were then anaesthetised and baroreflex sensitivity was measured following intravenous injection of phenylephrine (PE) and sodium nitroprusside (SNP) at various doses. Morphological changes of the brainstem were detected by transmission electron microscopy. Baroreflex sensitivity-associated gene and protein expression was determined by quantitative RT-PCR and Western blot analysis. We found that: (1) the HFCD significantly attenuated heart rate responses to arterial blood pressure (ABP) increases induced by PE, but had no effect on heart rate responses to ABP decreases induced by SNP; (2) the HFCD induced medullary sheath thickening, myelinated nerve atrophy and hyaloplasm dissolving; (3) protein levels of substance P, calcitonin gene-related peptide, GlutR2 and γ-aminobutyric acid A receptors were all markedly decreased in the brainstems of rats administered with the HFCD. These findings conclude that a HFCD could impair the baroreflex sensitivity of rats. Remodelled morphology and decreased neurotransmitters and receptors in the domains of the nucleus tractus solitarii and nucleus ambiguus are participating in this process.

Diet: Vagal neurons: Nucleus tractus solitarii: Nucleus ambiguus: Rats

Autonomic neuropathic dysfunctions are common complications both in type 1 and type 2 diabetic patients[1–3] and impairment of the baroreflex control of heart rate (HR) may possibly contribute to life-threatening arrhythmias and even sudden death, such as 'dead-in-bed syndrome'[4,5]. Many clinical and experimental studies have suggested that type 2 diabetes usually accompanies obesity (a modern disease associated with diet and lifestyle), and clinical as well as animal studies using obese animal models have demonstrated that obesity is an independent risk factor for CVD and impaired parasympathetic activity[6–11]. However, our knowledge on the mechanism of obesity-related changes in baroreflex sensitivity (BRS) remains fragmentary. In addition, although the individual impacts of high-fat and high-carbohydrate diets on BRS have been studied extensively[12–16], little is known about the combination effects and mechanisms of these two types of diets.

In order to provide integrative information about modern fast food and sedentary lifestyle, we examined the impact of complex high-fat and high-carbohydrate diet (HFCD) consumption on the BRS of Wistar rats. The formulated HFCD emulsion that was used in the present study contained lard, thyreostat, cholesterol, sucrose, fructose, sodium glutamate and salt. Lard and cholesterol were used to provide a high fat content; sucrose and fructose, which have been reported to be associated with the development of insulin resistance, were used to provide a high-carbohydrate food[17]. High salt, which is considered an independent risk factor of hypertension which is closely associated with diabetes, was also included in the diet[18]. Thyreostat, an anti-thyroid drug, was added in the formula to inhibit the metabolism of the animal, therefore mimicking the sedentary living habit.

Though both sympathetic and parasympathetic systems contribute to regulate heart function within the baroreflex circuitry, the parasympathetic system was thought to be the major pathway in baroreflex-mediated HR control[19]. Basically, the baroreflex is initiated by a rise in arterial blood pressure (ABP) that activates the afferent terminal located in the aortic arch and then transduction to afferent neurons in the nodose ganglia that project to nucleus tractus solitarii (NTS) neurons. Neurons in the NTS in turn activate cardioinhibitory vagal preganglionic neurons located primarily in the nucleus ambiguus (NA)[19,20]. The anatomical pathway of the baroreflex circuitry contains at least the following components: (1) cardiovascular mechanoreceptor-associated

Abbreviations: ABP, arterial blood pressure; BRS, baroreflex sensitivity; CGRP, calcitonin gene-related peptide; $GABA_A$, γ-aminobutyric acid A; HFCD, high-fat and high-carbohydrate diet; HR, heart rate; MABP, mean arterial blood pressure; NA, nucleus ambiguus; NTS, nucleus tractus solitarii; PE, phenylephrine; SNP, sodium nitroprusside; SP, substance P.

* **Corresponding author:** Dr Baofeng Yang, fax +86 451 86667511, email a.z.hrbmu@gmail.com

afferent neurons; (2) second-order NTS neurons; (3) cardiac parasympathetic preganglionic motor neurons located primarily in the NA; (4) parasympathetic postganglionic neurons intrinsic to the heart[19]. Within the baroreflex circuitry, the NTS and NA have been considered the central components that regulate the autonomic activities of the baroreflex[20]. A recent study has shown that lesions of the NTS lead to an increased probability of changes in ABP and sudden death in animals[21]. We hence aimed to explore whether the NTS and NA are involved in the impairment of BRS in rats receiving a HFCD.

Materials and methods

Preparation of the fat emulsion

The complex high-fat and high-carbohydrate diet (HFCD) emulsion was prepared as previously with minor changes[22]. The fat emulsion contained lard (20 %), thyreostat (1 %), cholesterol (5 %), sucrose (5 %), fructose (5 %), sodium glutamate (1 %) and salt (6 %) in 20 % Tween 80 and 30 % (v/v) propylene glycol. The diet was stored at 4°C before use.

Animals and treatment groups

Male Wistar rats (*n* 24, weight 200–230 g, aged about 3–4 months) were obtained from the Animal Centre of the 2nd Affiliated Hospital of Harbin Medical University (Harbin, Heilongjiang Province, China) and housed at 23 ± 1°C with 55 ± 5 % of humidity and a 12 h light–dark cycle. The use of animals was approved by the ethics committee of Harbin Medical University (no. HMUIRB-2008-06).

Rats were randomly divided into two groups with twelve rats per group. The HFCD group received the HFCD emulsion (10 ml/kg) by oral administration and the control group received 0·9 % NaCl (10 ml/kg) in 20 % Tween 80 and 30 % (v/v) propylene glycol. All rats were treated for 30 d.

Surgical procedure

Rats were anaesthetised with sodium pentobarbital (40 mg/kg) via intraperitoneal injection. Supplemental doses of anaesthetics (0·1 ml of 1 % sodium pentobarbital) were administered every 30 min to prevent eye blink and pedal-withdrawal reflexes. The tips of polyethylene-50 catheters were tapered to 0·5 mm in diameter. Following the exposure of the femoral artery (left) and the femoral vein (right), the tapered tips of two catheters filled with heparinised saline were then inserted into the femoral artery and vein, respectively. Vasoactive drugs were injected into the femoral vein and blood pressure was measured through the femoral artery.

Baroreflex sensitivity

The blood pressure catheter was connected to a blood pressure transducer (MlT0699; AD Instruments, Australia), which was positioned at heart level. ABP was measured automatically using the BL-420 Data Acquisition & Analysis System (Chengdu Tme Technology Co., Ltd, China). HR was calculated from pulse pressures using Ratemeter function. Injection of phenylephrine (PE) or sodium nitroprusside (SNP) was designed with different doses (PE: 16, 32, 64, 128 and 256 μg/ml; SNP: 10, 20, 40, 80 and 160 μg/ml with an injection speed of 0·04 ml/100 mg). A second drug administration was performed only when the former HR and ABP responses reached a plateau. The maximal HR responses relative to the HR baseline level (ΔHR) and mean ABP (MABP) changes relative to the ABP baseline level (ΔMABP) induced by injection of PE or SNP were recorded and analysed. BRS was then estimated by the calculated and averaged ratio of ΔHR:ΔMABP for each dosage of each drug. Dose-dependent curves of ΔHR:ΔMABP *v.* PE or SNP concentration were plotted for each group. Curves of ΔHR *v.* ΔMABP were also plotted to examine the maximal HR responses induced by MABP changes. All curves were fitted using the Boltzmann equation by Prism 5.0 software[23].

Transmission electron microscopy analysis

Locations of the NA and NTS were identified by a previously described protocol[24]. Transmission electron microscopy analysis was performed as follows: animals in each group were anaesthetised with sodium pentobarbital (100 mg/kg) and perfusion with 0·9 % saline and 10 % phosphate-buffered (pH 7·4) formalin. The NTS and NA were removed and immersed in a stationary liquid (pH 7·3) containing 3 % glutaraldehyde in 0·1 M-sodium phosphate buffer and 0·45 M-Ca^{2+}. Tissue samples were then post-fixed in 2 % OsO_4 phosphate buffer containing 1·5 % potassium ferricyanide. After dehydration in a graded concentration of alcohol, tissues were then embedded in Epon with propylene oxide as an intermediary solvent. Plastic sections (1 μm thick) were stained with toluidine blue and examined under a light microscope. Ultrathin sections of tissues were mounted on formvar-coated slot grids, stained with uranyl acetate and lead citrate, and examined with a JEOL 1200 electron microscope (JEOL Co., Tokyo, Japan).

Quantitative RT-PCR analysis

Total RNA were prepared from rat brainstems (±600 μm from 0 point), and relative mRNA expression levels for substance P (SP; forward ACAGATTCCTTTGTTGG; reverse GCCTTCTTTCGTAGTTC), calcitonin gene-related peptide (CGRP; forward CCCTTTCCTGGTTGTCA; reverse CTCAGCCTCCTGTTCCTC), α-amino-3-hydroxy-5-methyl-4-isoxazole propionate (AMPA) receptor subunit 2 (GluR2; forward TGTCCTCCTTTCTCCCT; reverse CTGAACCATC-CCTACCC) and γ-aminobutyric acid A ($GABA_A$) receptor (forward CTGAAGTGAAGACGGACAT; reverse ACGCAG-GAGTTTATTGG) were measured by one-step real-time RT-PCR using the SYBR Green PCR Master Mix Kit (Ambion, Austin, TX, USA) on a 7500 FAST Real-Time PCR System (Applied Biosystems, Foster City, CA, USA).

Western blot analysis

The expression levels of proteins in brainstem tissues (±600 μm from 0 point) were detected by Western blot analysis. The proteins included in the present study were SP (11 kDa), CGRP (13 kDa), GluR2 (88 kDa) and $GABA_A$ (70 kDa). The primary antibodies and horseradish

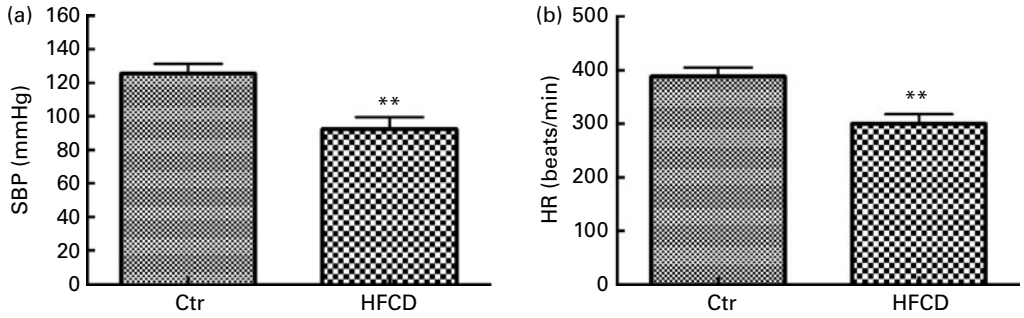

Fig. 1. Baseline systolic blood pressure (SBP) and heart rate (HR) in control rats (Ctr; *n* 7) and in rats fed a high-fat and -carbohydrate diet (HFCD; *n* 8). Values are means, with standard errors represented by vertical bars. ** Mean value was significantly different from that of the control group ($P<0{\cdot}01$).

peroxidase-conjugated secondary antibodies were all purchased from Santa Cruz Biotechnology (Santa Cruz, CA, USA).

Tissues were lysed with 600 μl lysis buffer containing 1 % protease inhibitor solution, and then centrifuged at 12 000 ***g*** per min for 30 min to collect protein extracts in the supernatant fraction. The protein concentration was determined by a Sunrise-Basic Tecan microplate reader (Tecan, Saltzberg, Austria) using bovine serum albumin as the standard. Protein samples were resolved on a 10 % SDS-PAGE gel and transferred to a polyvinylidene fluoride (PVDF) membrane (Bio-Rad, Hercules, CA, USA). The PVDF membrane was then incubated with the indicated primary antibodies diluted at 1:3000 in PBS buffer for 1 h at room temperature. The inhibitory peptide was used for each antibody to determine the antibody specificity. After being washed in PBS–Tween 20 (PBS-T) three times (10 min each), the membranes were incubated with horseradish peroxidase-conjugated secondary antibodies diluted at 1:5000 in PBS-T blocking buffer containing 5 % dry milk for 1 h at room temperature, followed by detection with the Odyssey IR imaging system (LI-COR Biosciences, Lincoln, NB, USA). β-Actin at 1:10 000 was used as the loading control for equal input of protein samples. The SDS-PAGE gel was stained with Coomassie blue solution before the transfer to verify the quantity of protein samples. Densitometry analysis was performed with Quantity One software (Bio-Rad) – area × optical density. The density of each protein was normalised with that of β-actin, and the expression levels of target proteins were expressed as fold changes over the expression of the control samples.

Statistical analysis

Data were analysed by one-way ANOVA. The significant difference was set as $P<0{\cdot}05$. Data were presented as the mean values with their standard errors and plotted using GraphPad Prism 5.0 software (GraphPad Software Inc., San Diego, CA, USA). Comparison between two groups was performed using Student's *t* test.

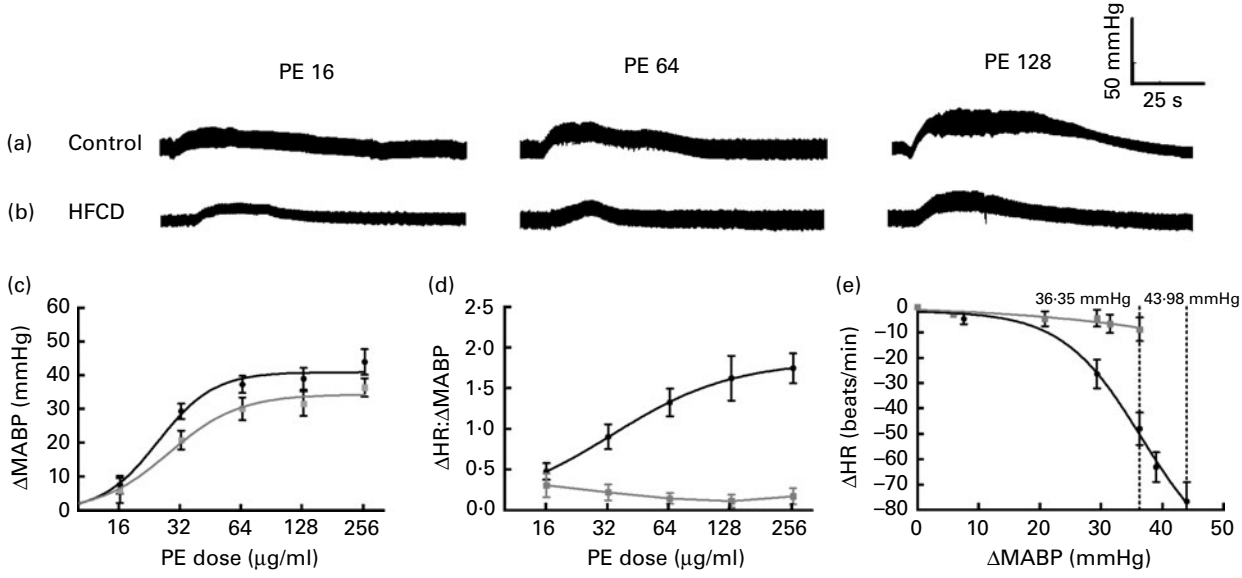

Fig. 2. Significant attenuation of baroreflex sensitivity by a high-fat and -carbohydrate diet (HFCD) following phenylephrine (PE) administration. Traces of blood pressure changes induced by PE application at 16, 64 and 128 μg/ml in (a) a rat fed the normal diet (control) and (b) a rat fed the HFCD. (c) The dose-dependent curve of HFCD rats (–■–) of change in mean arterial blood pressure (ΔMABP) against each dose of PE shifted to the right of the curve of control rats (–●–) (ANOVA; $P<0{\cdot}01$). (d) The dose-dependent change in heart rate (ΔHR):ΔMABP curve of HFCD rats shifted to the right of the curve of control rats (ANOVA; $P<0{\cdot}01$). (e) The ΔHR:ΔMABP curve of HFCD rats was plotted by ΔHR *v.* ΔMABP at each dose, and shifted to the right of the curve of control rats (ANOVA; $P<0{\cdot}01$). Values are means (*n* 6), with standard errors represented by vertical bars.

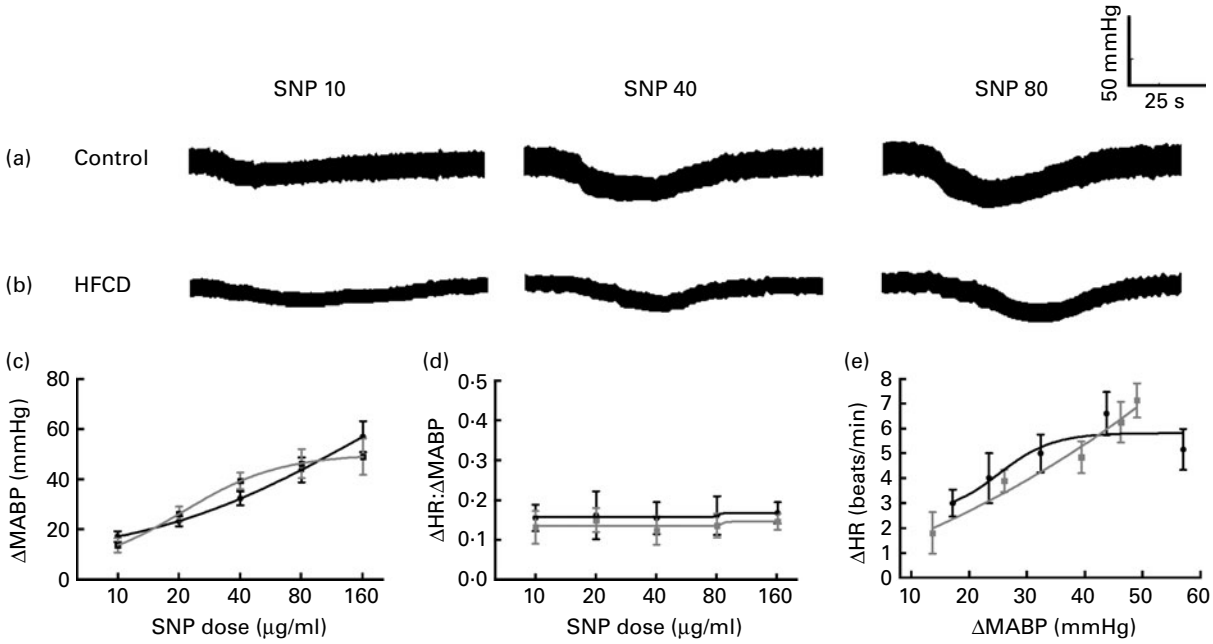

Fig. 3. Effect on baroreflex sensitivity of a high-fat and -carbohydrate diet (HFCD) during sodium nitroprusside (SNP) application. Traces of blood pressure changes induced by SNP application at 10, 40 and 80 μg/ml in (a) a rat fed the normal diet (control) and (b) a rat fed the HFCD. (c) Dose-dependent curve of HFCD rats (–■–) of change in mean arterial blood pressure (ΔMABP) against each dose of SNP. There was no significant difference between the HFCD group and the control group (–●–) (ANOVA; $P>0{\cdot}05$). (d) Dose-dependent change in heart rate (ΔHR):ΔMABP curve of HFCD rats, showing a similar pattern to that of control rats (ANOVA; $P>0{\cdot}05$). (e) ΔHR:ΔMABP curve of HFCD was plotted by ΔHR *v.* ΔMABP at each dose and no difference was observed between the control and treatment groups (ANOVA; $P>0{\cdot}05$). Values are means (n 6), with standard errors represented by vertical bars.

Results

Effects of high-fat and high-carbohydrate diet on systolic blood pressure and heart rate in anaesthetised rats

After rats were anaesthetised by sodium pentobarbital, baseline systolic blood pressure (SBP) and HR were measured before PE and SNP were applied. In control rats, SBP and HR were 121·23 (SEM 4·55) mmHg and 373·5 (SEM 7·83) beats/min, respectively. However, in HFCD-treated animals, the SBP and HR were reduced to 91·87 (SEM 7·58) mmHg and 294·83 (SEM 17·36) beats/min, respectively. Compared with the control group, SBP and HR in the HFCD-treated group were significantly reduced by 24 and 21 %, respectively (both $P<0{\cdot}01$; Fig. 1(a) and (b)).

Baroreflex control of heart rate during phenylephrine application

With the increase of PE doses, MABP increased gradually in both the normal diet-fed rats and HFCD-treated rats (Fig. 2(a) and (b)). However, compared with the control rats, the increase of ΔMABP following PE injection was markedly lower in the HFCD-treated rats, especially at PE dosages of 32, 64 and 128 μg/ml (Fig. 2(c); ANOVA; $P<0{\cdot}01$). As an index of BRS, ΔHR:ΔMABP values were significantly decreased in HFCD-treated rats receiving PE at 32, 64, 128 and 256 μg/ml than in control rats (Fig. 2(d)). The maximal ΔHR in response to the maximal ΔMABP was also significantly attenuated in HFCD-treated rats (Fig. 2(e)).

Baroreflex control of heart rate during sodium nitroprusside application

SNP induced the decrease of MABP in a dose-dependent manner (Fig. 3(a) and (b)). However, no significant differences of ΔMABP were observed between the control and HFCD-treated rats (Fig. 3(c); ANOVA; $P>0{\cdot}10$). SNP dose-dependent curves of BRS (ΔHR:ΔMABP) and the response of maximal ΔHR to the maximal ΔMABP were plotted and showed a similar pattern in both groups (Fig. 3(d) and (e); ANOVA; $P>0{\cdot}10$).

Ultrastructural remodelling of nucleus tractus solitarii and nucleus ambiguus

Compared with control rats, the dilatation of the endoplasmic reticulum, mitochondrion and Golgi body complex as well as damaged membrane structures of mitochondria were frequently found in both the NTS (Fig. 4(a), (b), (c) and (d)) and NA (data not shown here) domains of the HFCD-treated rats. In addition, for myelinated nerve fibres, medullary sheath thickening, nerve atrophy and axoplasm dissolving were also observed (Fig. 4(e) and (f)).

Evaluation of baroreflex-related mRNA and protein expression

SP and CGRP in the NTS and NA are two key peptides in the baroreflex circuitry[25,26]. The present results showed that compared with control rats, the mRNA levels of both SP and CGRP in HFCD-treated rats were increased by 1·78 (SEM 0·06) and 2·0 (SEM 0·05) fold, respectively (Fig. 5(a)

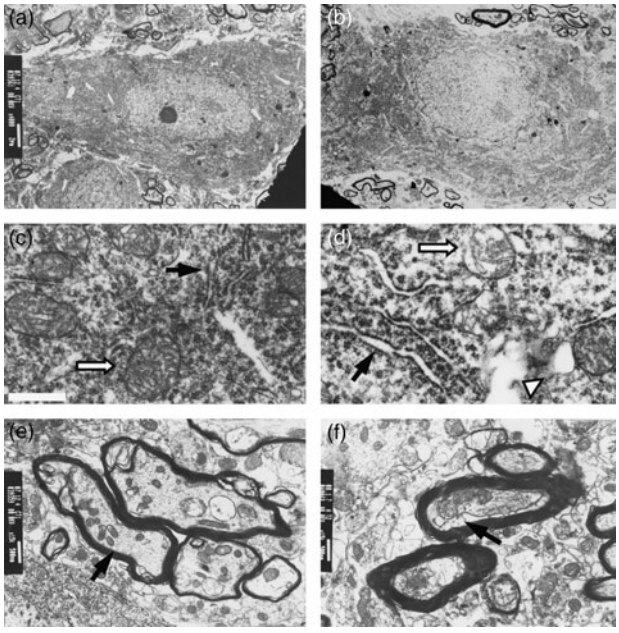

Fig. 4. Electron micrographs of the ultrastructural characteristics of the nucleus tractus solitarii (NTS) in high-fat and -carbohydrate diet (HFCD)-treated and untreated rats. (a) Electron micrograph of a neuron from the NTS domain in a normal rat. A large nucleus in the centre of a large neuron with a clear boundary is shown. (b) Electron micrograph of a neuron from the NTS domain in a HFCD-treated rat. The same structure as in (a) is shown with a decreased electron density of the nucleus. (c) Electron micrograph of the cytoplasm from the NTS domain in a normal rat. The normal structures of mitochondria and endoplasmic reticulum are indicated by a white arrow and a black arrow, respectively. (d) Electron micrograph of the cytoplasm from the NTS domain in a HFCD-treated rat. The expanded endoplasmic reticulum is indicated by a black arrow and a white triangle; an expanded mitochondrion and damaged membrane structure are indicated by a white arrow. (e) Electron micrograph of the ultrastructure of myelinated nerves from the NTS domain in a normal rat. Microtubules, microfilaments and neurofilaments fill up the medullary sheath and the membrane of myelinated nerves is attached tightly to the inner wall of the medullary sheath (indicated by a black arrow). (f) Electron micrograph of myelinated nerves from the NTS domain in a HFCD-treated rat. Increased thickness of medullary sheaths and enlarged interspaces between the axolemma and medullary sheaths are indicated by an arrow. Scale bar: 4 μm in (a) and (b); 1 μm in c, (d), (e) and (f).

and (b); $P<0{\cdot}05$). However, protein levels of SP and CGRP in the brainstem of HFCD-treated rats were significantly decreased by 0·68 (SEM 0·03) and 0·65 (SEM 0·01) fold, respectively (Fig. 5(e) and (f); $P<0{\cdot}05$), indicating that post-transcriptional changes of the two peptides may be a mechanism of baroreflex dysfunction in HFCD-treated rats. Glutamate is the major excitatory neurotransmitter in the NTS and evokes decreases in blood pressure and HR via activating non-*N*-methyl-D-aspartate (NMDA) receptors, such as GlutR2, a subunit of α-amino-3-hydroxy-5-methyl-4-isoxazole propionate (AMPA) receptors[27]. In HFCD-treated rats, although its mRNA level was not significantly altered (Fig. 5(c); $P>0{\cdot}05$), the protein level of GlutR2 was significantly decreased (0·46 (SEM 0·03) fold; Fig. 5(g); $P<0{\cdot}05$) compared with that of the control rats. GABA functions as a major central nervous system inhibitory transmitter via $GABA_A$ receptors within the NTS[28]. Compared with control animals, HFCD-fed rats showed 0·86 (SEM 0·01) and 0·74 (SEM 0·1) fold decreases of GABA at the mRNA and protein levels in the brainstem, respectively (Fig. 5(d) and (h); $P<0{\cdot}05$).

Discussion

In the present study, in order to mimic the routine human lifestyle of modern society, we first formulated a HFCD emulsion containing both high-fat and high-carbohydrate food. The HFCD emulsion was administered to rats by oral administration but not by food feeding so as to control the daily HFCD intake. In this way, the possible imbalance of fat intake due to decreased appetite as a result of a high-fat diet was avoided[22]. Our previous study has demonstrated that the complex HFCD can induce arrhythmia, reduce both systolic and diastolic functions of the heart, and lead to morphological remodelling and related protein expression changes in cardiomyocytes in rats (data not shown). Heart function is strongly regulated by the central nervous system, especially by the parasympathetic and sympathetic system. Here we show that the HFCD could also impair the sensitivity of baroreflex control of the HR and induce remodelling of the ultrastructure of both cell organelles and medullary sheaths in the brainstem. Moreover, protein expressions of SP, CGRP, GlutR2 and $GABA_A$ receptors were all markedly decreased by the HFCD.

High-fat and high-carbohydrate diet decreases blood pressure and heart rate in anaesthetised rats

In the present study, we first reported that it was hypotension but not hypertension that was observed in anaesthetised HFCD-treated rats. This result differs from those of previous studies which described either hypertension or no change in high-fat-induced obese rats[29–31]. The change may be based on: (1) the discrepancies between the direct and indirect blood pressure measurement or intervention duration[29,31]; (2) sodium pentobarbital could inhibit cardiac output more than when animals are in the conscious resting state[32]; (3) obesity was associated with reduced vascular compliance as well as higher stiffness index[33]. We hence speculated that the hypotension in HFCD-treated rats under an anaesthetic state may be associated with decreased cardiac output combined with reduced vascular compliance. However, what the exact mechanism is that led to hypotension in HFCD-treated rats under the anaesthetic state is an interesting issue that deserves further investigation.

High-fat and high-carbohydrate diet reduces baroreflex control of heart rate and remodels the structure of nucleus tractus solitarii and nucleus ambiguus

Our data showed that baroreflex control of the HR in complex HFCD-treated anaesthetised rats was significantly reduced by PE but not by SNP at all given doses. This observation indicates that there might be two distinct pathways to regulate the increase and decrease of blood pressure individually[23,33]. Though we did not observe significant effects of the HFCD on the HR response to SNP, the result may not conclude that the HFCD did not affect it. Detection in conscious rats would be the best way to evaluate the actions of the HFCD on the baroreflex circuitry.

Mitochondria are the central organelles for the oxidative synthesis of ATP and play a critical role in the regulation of cell functions[34]. Mitochondrial abnormalities may lead to insufficient energy supply for cell production and cytolergy,

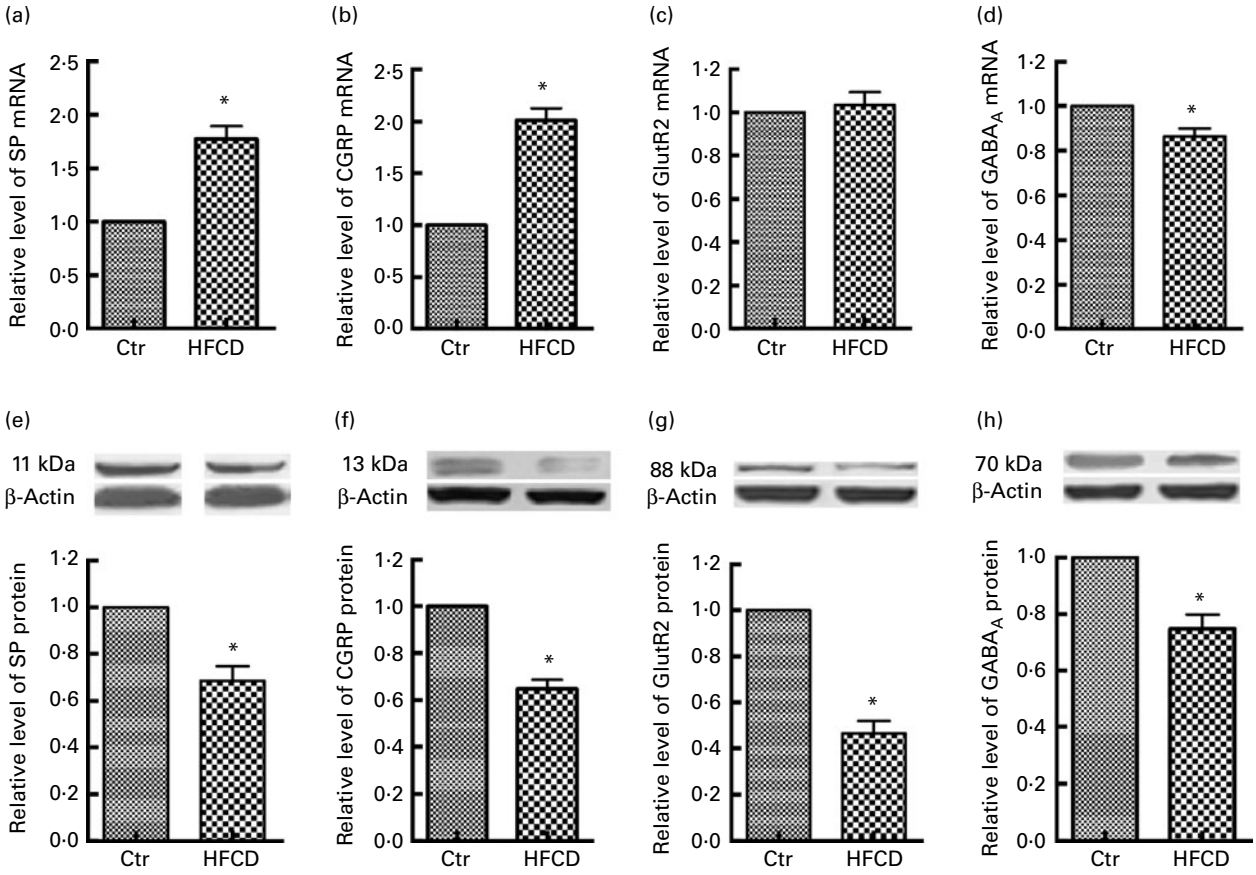

Fig. 5. Baroreflex-related mRNA and protein expression in high-fat and -carbohydrate diet (HFCD)-treated and control (Ctr) rats. Relative mRNA and protein levels of substance P (SP) (a and e), calcitonin gene-related peptide (CGRP) (b and f), GlutR2 (c and g) and γ-aminobutyric acid A ($GABA_A$) (d and h). Western blot results are also shown in (e), (f), (g) and (h). Values are means of six independent experiments, with standard errors represented by vertical bars. * Mean value was significantly different from that of the control ($P<0·05$).

such as protein synthesis and modification in the endoplasmic reticulum and Golgi complex, respectively[35]. The dilatation of the endoplasmic reticulum and Golgi complex observed in the present study may be a consequence of damaged mitochondria or increased NEFA induced by the complex HFCD. The baroreflex pathway begins with the cardiovascular mechanoreceptors of afferent neurons, including A-type receptors with rapidly conducting myelinated fibres and C-type receptors with lower conducting unmyelinated axons. A-type conducting myelinated fibres exert the predominant function in the baroreflex circuitry[19]. As we know, myelination helps prevent the electrical current from leaving the axon and the main purpose of a medullary sheath is to increase the speed at which impulses propagate along the myelinated fibre. Abnormal myelination, including myelin sheath atrophy or thickening, can induce dysfunction of the myelin sheath insulating the nerves and even reduce the propagation of impulses along the myelinated fibre.The results suggest that the complex HFCD-induced attenuation of BRS may be associated with remodelled myelin sheaths in A-type nerves.

Molecular mechanisms of high-fat and high-carbohydrate diet action on normal rats

SP and CGRP have been reported to enhance the release of glutamate and hence modulate glutamatergic transmission. Consequently, blood pressure is decreased through the action of glutamate on GlutR2[27,36]. Our finding that SP, CGRP and GlutR2 protein levels were all decreased in HFCD-treated rats suggests that the impaired BRS in these animals may be due to the reduction in SP, CGRP and GlutR2 functions. GABA increases the blood pressure by inhibiting the parasympathetic system within the NTS via $GABA_A$ receptors[28,37], and decreased protein expression of $GABA_A$ receptors in HFCD rats implies that the reduction of GABAergic function may be another mechanism by which the HFCD impairs BRS.

In summary, the results provided basic study evidence to suggest that long-term HFCD application would be a risk factor to induce the onset of cardiac sudden death by attenuated BRS.

Acknowledgements

This research was supported by grants from the Key Project of Natural Science Foundation of Heilongjiang Province (no. ZJY0703-02), National Basic Research Program of China (973 program; no. 2007CB512006), Natural Science Foundation of China (no. 30870862), New Century Excellent Talents in Universities, Chinese Ministry of Education and Chinese Ministry of Education (no. NCET-08) and Specialized Research Fund for Science and Technology Creative

Research Talents by Harbin Science and Technology Bureau (no. 2008RFLXS009).

J. A. and B.Y. supervised the project and wrote the manuscript; F. L. and J. Z. performed the animal studies including blood pressure, HR and BRS recording; N. W. and S. Z. designed and performed real-time quantitative RT-PCR; H. Z. and J. A designed and conducted the Western blot analysis.

We thank Li Zhang and Yueming Chi for technical support for handling the transmission electron microscopy machine.

None of the authors had a conflict of interest.

References

1. Ziegler D (1994) Diabetic cardiovascular autonomic neuropathy: prognosis, diagnosis and treatment. *Diabetes Metab Rev* **10**, 339–383.
2. Dall'Ago P, D'Agord Schaan B, da Silva VOK, *et al.* (2007) Parasympathetic dysfunction is associated with baroreflex and chemoreflex impairment in streptozotocin-induced diabetes in rats. *Auton Neurosci* **131**, 28–35.
3. Movahed MR (2007) Diabetes as a risk factor for cardiac conduction defects: a review. *Diabetes Obes Metab* **9**, 276–281.
4. Bell DS (2006) "Dead in bed syndrome": a hypothesis. *Diabetes Obes Metab* **8**, 261–263.
5. Weston PJ & Gill GV (1999) Is undetected autonomic dysfunction responsible for sudden death in type 1 diabetes mellitus? The 'dead in bed' syndrome revisited. *Diabet Med* **16**, 626–631.
6. Skrapari I, Tentolouris N, Perrea D, *et al.* (2007) Baroreflex sensitivity in obesity: relationship with cardiac autonomic nervous system activity. *Obesity (Silver Spring)* **15**, 1685–1693.
7. Skrapari I, Tentolouris N & Katsilambros N (2006) Baroreflex function: determinants in healthy subjects and disturbances in diabetes, obesity and metabolic syndrome. *Curr Diabetes Rev* **2**, 329–338.
8. Sowers JR (2003) Obesity as a cardiovascular risk factor. *Am J Med* **115**, 37S–41S.
9. Brunner EJ, Mosdøl A, Witte DR, *et al.* (2008) Dietary patterns and 15-y risks of major coronary events, diabetes, and mortality. *Am J Clin Nutr* **87**, 1414–1421.
10. Van Vliet BN, Hall JE, Mizelle HL, *et al.* (1995) Reduced parasympathetic control of heart rate in obese dogs. *Am J Physiol* **269**, H629–H637.
11. Schreihofer AM, Mandel DA, Mobley SC, *et al.* (2007) Impairment of sympathetic baroreceptor reflexes in obese Zucker rats. *Am J Physiol Heart Circ Physiol* **293**, H2543–H2549.
12. Chess DJ & Stanley WC (2008) Role of diet and fuel overabundance in the development and progression of heart failure. *Cardiovasc Res* **79**, 269–278.
13. Schutte AE, Van Rooyen JM, Huisman HW, *et al.* (2006) Modulation of baroreflex sensitivity by walnuts versus cashew nuts in subjects with metabolic syndrome. *Am J Hypertens* **19**, 629–636.
14. Halton TL, Willett WC, Liu S, *et al.* (2006) Low-carbohydrate-diet score and the risk of coronary heart disease in women. *N Engl J Med* **55**, 1991–2002.
15. Straznicky NE, Lambert GW, Masuo K, *et al.* (2009) Blunted sympathetic neural response to oral glucose in obese subjects with the insulin-resistant metabolic syndrome. *Am J Clin Nutr* **89**, 27–36.
16. Madden KM, Tedder G, Lockhart C, *et al.* (2008) Oral glucose tolerance test reduces arterial baroreflex sensitivity in older adults. *Can J Physiol Pharmacol* **86**, 71–77.
17. Pénicaud L, Berthault MF, Morin J, *et al.* (1998) Rilmenidine normalizes fructose-induced insulin resistance and hypertension in rats. *J Hypertens Suppl* **16**, S45–S49.
18. Yang G (2009) Salt intake in individuals with metabolic syndrome. *Lancet* **373**, 792–794.
19. Andresen MC, Kunze DL & Mendelowitz D (2004) Central nervous system regulation of the heart. In *Basic and Clinical Neurocardiology*, pp. 187–219 [JA Armour and JL Ardell, editors]. New York: Oxford University Press.
20. Cheng Z, Zhang H, Yu J, *et al.* (2004) Attenuation of baroreflex sensitivity after domoic acid lesion of the nucleus ambiguus of rats. *J Appl Physiol* **963**, 1137–1145.
21. Nayate A, Moore SA, Weiss R, *et al.* (2009) Cardiac damage after lesions of the nucleus tractus solitarii. *Am J Physiol Regul Integr Comp Physiol* **296**, R272–R279.
22. Ai J, Wang N, Yang M, *et al.* (2005) Development of Wistar rat model of insulin resistance. *World J Gastroenterol* **11**, 3675–3679.
23. Lin M, Liu R, Gozal D, *et al.* (2007) Chronic intermittent hypoxia impairs baroreflex control of heart rate but enhances heart rate responses to vagal efferent stimulation in anesthetized mice. *Am J Physiol Heart Circ Physiol* **293**, H997–H1006.
24. Ai J, Epstein PN, Gozal D, *et al.* (2007) Morphology and topography of nucleus ambiguus projections to cardiac ganglia in rats and mice. *Neuroscience* **149**, 845–860.
25. Haeusler G & Osterwalder R (1980) Evidence suggesting a transmitter or neuromodulatory role for substance P at the first synapse of the baroreceptor reflex. *Naunyn Schmiedebergs Arch Pharmacol* **314**, 111–121.
26. Franco-Cereceda A (1988) Calcitonin gene-related peptide and tachykinins in relation to local sensory control of cardiac contractility and coronary vascular tone. *Acta Physiol Scand* **569**, 2–63.
27. Lin LH, Taktakishvili OM, Talman WT, *et al.* (2008) Colocalization of neurokinin-1-*N*-methyl-D-aspartate, and AMPA receptors on neurons of the rat nucleus tractus solitarii. *Neuroscience* **154**, 690–700.
28. Erdos B, Broxson CS, Cudykier I, *et al.* (2009) Effect of high-fat diet feeding on hypothalamic redox signaling and central blood pressure regulation. *Hypertens Res* **32**, 983–988.
29. Nagae A, Fujita M, Kawarazaki H, *et al.* (2009) Effect of high fat loading in Dahl salt-sensitive rats. *Clin Exp Hypertens* **31**, 451–461.
30. Janssen BJ, De Celle T, Debets JJ, *et al.* (2004) Effects of anesthetics on systemic hemodynamics in mice. *Am J Physiol Heart Circ Physiol* **287**, H1618–H1624.
31. Millis RM, Austin RE, Bond V, *et al.* (2009) Effects of high-carbohydrate and high-fat dietary treatments on measures of heart rate variability and sympathovagal balance. *Life Sci* **85**, 141–145.
32. Robinson MR, Scheuermann-Freestone M, Leeson P, *et al.* (2008) Uncomplicated obesity is associated with abnormal aortic function assessed by cardiovascular magnetic resonance. *J Cardiovasc Magn Reson* **10**, 10.
33. Murphy AZ, Ennis M, Rizvi TA, *et al.* (1995) Fos expression induced by changes in arterial pressure is localized in distinct, longitudinally organized columns of neurons in the rat midbrain periaqueductal gray. *J Comp Neurol* **360**, 286–300.
34. Henderson LA, Richard CA, Macey PM, *et al.* (2004) Functional magnetic resonance signal changes in neural structures to baroreceptor reflex activation. *J Appl Physiol* **96**, 693–703.
35. Orth M & Schapira AH (2001) Mitochondria and degenerative disorders. *Am J Med Genet* **106**, 27–36.
36. Van Giersbergen PLM, Palkovits M, De Jong W, *et al.* (1992) Involvement of neurotransmitters in the nucleus tractus solitarii in cardiovascular regulation. *Physiol Rev* **2**, 789–824.
37. Jacob TC, Moss SJ, Jurd R, *et al.* (2008) $GABA_A$ receptor trafficking and its role in the dynamic modulation of neuronal inhibition. *Nat Rev Neurosci* **9**, 331–343.